Microelectronics Reliability 126 (2021) 114322

Contents lists available at ScienceDirect

Microelectronics Reliability

journal homepage: www.elsevier.com/locate/microrel

Recharging process of commercial floating-gate MOS transistor in dosimetry application

Stefan D. Ilić [a,b], Marko S. Andjelković [c], Russell Duane [d], Alberto J. Palma [e], Milija Sarajlić [b], Srboljub Stanković [f], Goran S. Ristić [a,*]

[a] Applied Physics Laboratory, Faculty of Electronic Engineering, University of Niš, Serbia
[b] Center of Microelectronic Technologies, Institute of Chemistry, Technology and Metallurgy, University of Belgrade, Serbia
[c] System Architectures Department, IHP - Leibniz-Institut für innovative Mikroelektronik, Frankfurt (Oder), Germany
[d] Centre for Micro and Nano Systems, Tyndall National Institute, University College Cork, Dyke Parade, Cork, Ireland
[e] Department of Electronics and Computer Technology, University of Granada, Granada, Spain
[f] Department of Radiation and Environmental Protection, "Vinča" Institute of Nuclear Sciences, University of Belgrade, Serbia

ARTICLE INFO

Keywords:
Floating gate
Radiation sensor
EPAD
Recharging
Programming cell
Non-volatile memory

ABSTRACT

We investigated the recharging process of commercial floating gate device (EPAD) during the six different dose rates and ten irradiation cycles with the highest dose rate. Dose rate dependence of the floating gate dosimeter was observed from 1 Gy/h to 26 Gy/h (H_2O). There is no change of the dosimetric characteristic with a constant dose rate of 26 Gy/h for ten cycles. The absorbed dose does not affect the drift of the threshold voltage readings after the irradiation steps. The reprogramming characteristic is not degrading with the absorbed dose for the ten irradiation cycles, giving the promising potential in the application for dosimetric purposes.

1. Introduction

Different types of ionizing radiation-sensitive dosimeters have emerged during the development of technology from traditional thermoluminescent detectors [1], through radiation field effect transistors (RadFET-s) [2–4], ionizing chamber based dosimeters [5,6], MOS-capacitance based sensor [7] and floating gate structures [8–11]. Special floating gate sensor with zero bias operation and reprogramming capabilities has been designed in a standard 0.6 μ CMOS technology by the group of authors from CERN in collaboration with IC Malaga [12–15].

A specific commercial component that has an n-channel MOS transistor with a floating gate called Electrically Programmable Analog Device (EPAD) is a product of Advanced Linear Devices, Inc. An EPAD has an exceptional adjustment of threshold voltage value, and it is designed for matched-pair balanced circuit configurations, such as current sources and current mirrors and in all applications where precise voltage adjustment is needed. A group of authors from United Kingdom used this device as a radiation dosimeter [16,17].

Realising the floating gate dosimeter's great potential, we based our research on the ALD1108E integrated circuit, which consists of four EPADs on a chip manufactured by the same company [18]. So far, we have investigated the sensitivity of EPADs to gamma radiation with zero, static and dynamic bias at the control gate, the effect of absorbed dose and gate biasing on reprogramming characteristic, spontaneous recovery and annealing after irradiation [19,20]. The impact of reprogramming EPAD between irradiation phases has not been investigated so far. This paper aims to examine the behavior of floating gate MOS transistor during the irradiation and reprogramming cycles for the same and different dose rates and whether a commercial component intended for entirely different purposes can achieve the level requirements of a professional dosimeter.

2. Electrically programmable analog device

The EPAD structure consists of a main and a charging transistor; they have a common floating and control gate, as shown in Fig. 1.

The floating gate is surrounded by oxide. Between control and a floating gate, there is interpoly oxide, and between the floating gate and substrate, there is field oxide. The floating gate has a large area above the thick (field) oxide whose role is to be a large reservoir of electrons, as well as that the charge stored at the floating gate does not leak over time

* Corresponding author at: Applied Physics Laboratory, Faculty of Electronic Engineering, University of Niš, Serbia.
E-mail addresses: stefan.ilic@nanosys.ihtm.bg.ac.rs (S.D. Ilić), goran.ristic@elfak.ni.ac.rs (G.S. Ristić).

https://doi.org/10.1016/j.microrel.2021.114322
Received 22 May 2021; Received in revised form 6 July 2021; Accepted 23 July 2021
Available online 11 October 2021

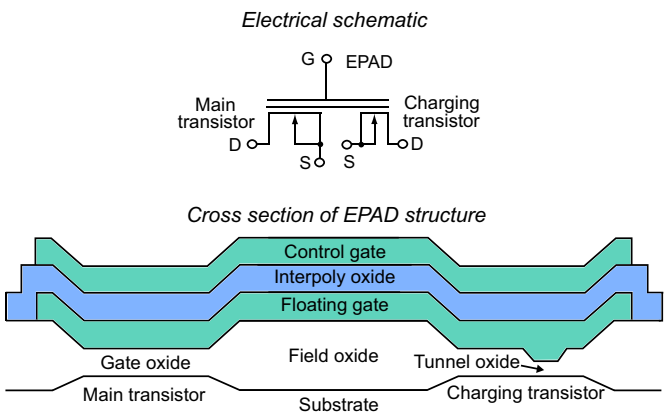

Fig. 1. Electrical schematic and cross section of EPAD structure.

so that the device has a stable threshold voltage value.

The charging transistor has a thin oxide (tunnel oxide), and its role is to be used for charging the floating gate with electrons (programming). Electrons are attracted from the charging transistor's channel to the floating gate by a strong electric field from the control gate. All residual charge that can remain in the tunnel oxide traps or at the interface between the oxide and the channel after the programming does not affect the main transistor, which gives a great advantage to this structure because monitoring and charging processes are separated. Another advantage of this structure is the thick field oxide below the floating gate that will generate a large amount of electron-hole pairs because the radiation-generated charge depends on the oxide thickness during irradiation [21]. Basic three mechanisms which could cause a threshold voltage decrease (shift) during irradiation [22] are shown in the energy band diagram of the EPAD structure with charged floating gate (Fig. 2).

The coloured numbers in parentheses in Fig. 2 denote the following mechanisms [22]:

1. Injection into the floating gate of the positive charge generated by ionizing radiation in the field and interpoly oxide (surrounding oxides). Since the field oxide is much thicker, its influence on the generation of electron-hole pairs is much greater than interpoly oxide.

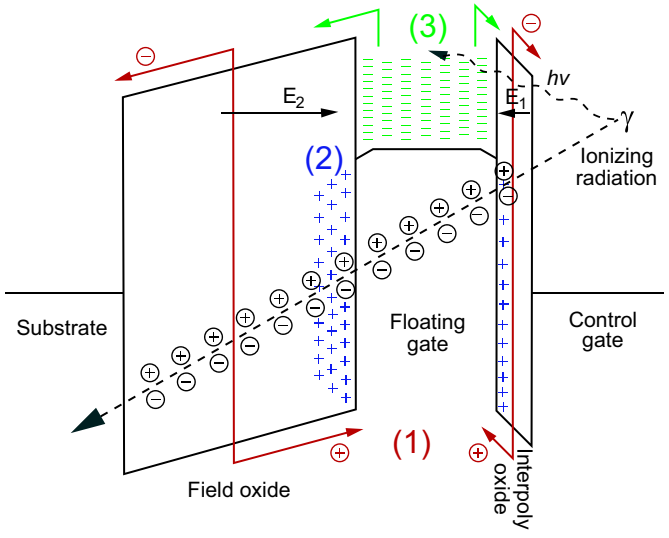

Fig. 2. Three mechanisms responsible for threshold voltage shift during irradiation shown in the energy band diagram of the EPAD structure with charged floating gate.

2. Positive charge trapping in the surrounding oxides. As shown in the Fig. 2, a larger amount of trapped charge remains in the field oxide near the floating gate than in the interpoly oxide because of its different thicknesses. In the first and second mechanism, electrons as faster particles compared to holes under the influence of an electric field from the floating gate are blown away towards the substrate or the control gate where they recombine. Although the first two mechanisms are physically different, from the engineering perspective, the amount of charge in the floating gate and its surroundings is reduced by direct recombination as in the first mechanism, or its electric field is neutralized in the second mechanism.
3. Photoemission. Electron emission over the polysilicon/oxide barriers. Captured electrons in a floating gate receive enough energy from high-energy photons to surmount the potential barrier and become free by reducing the floating gate charge.

Described mechanisms apply to all floating gate devices, but floating gate memories differ from the EPAD, since their design has no field oxide and large floating gate area, and therefore their sensitivity to ionizing radiation is much lower [23].

3. Initial programming of floating gate structure

All EPADs are programmed at the factory to the threshold voltage value of 1 V. Initial programming characteristics before irradiation from 1 V to 4 V are shown in Fig. 3.

It can be noted that all EPADs have the same dependence of the programming time required to shift the threshold voltage, but there is a large range of programming time that is varying even at the same chip. Based on a large number of samples, it was obtained that programming time can vary from 15 to 38 min for 1 V to 4 V threshold voltage shift.

Sub-threshold characteristics of EPAD at approximately equidistant steps during programming are shown in Fig. 4. Analysing the subthreshold characteristics for the main transistor, it is found that the slope does not change during the programming process, indicating no residual charges at the interface between the oxide and the channel. Software for analysing was written in GNU Octave [24]. It is based on midgap subthreshold technique used for separation of oxide, and interface traps of subthreshold characteristics of MOS transistors [25]. Unfortunately, this software cannot distinguish the charge on the floating gate and electrons trapped in the oxide.

Threshold voltage drift after programming process for two EPADs on the same chip is shown in Fig. 5.

It is observed that the threshold voltage value decreases over time

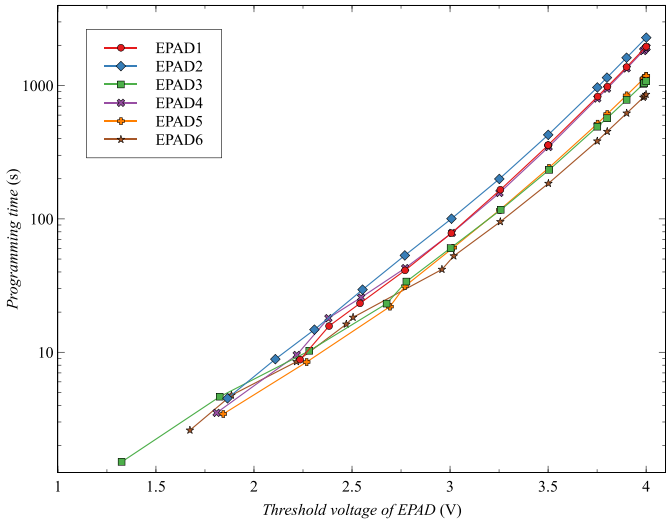

Fig. 3. Programming characteristics of EPADs.

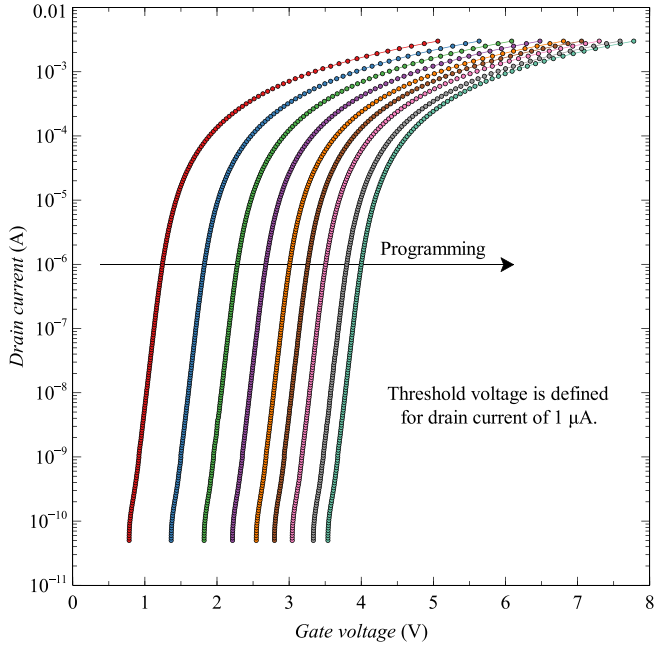

Fig. 4. Sub-threshold characteristics of EPAD during programming.

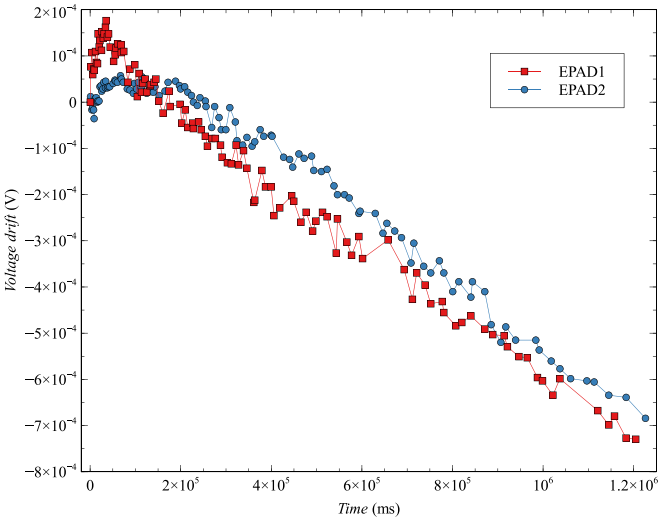

Fig. 5. Threshold voltage drift of EPADs after programming process.

after programming because there are residual electrons that can gain sufficient energy to become detrapped. We assume that these electrons are at the boundary between the oxide and the floating gate (polysilicon). Relaxation time is typically about 2 h after the programming for ALD1108E [26].

4. Recharging of floating gate in radiation dosimetry

The experiment was performed using a Co-60 gamma radiation source in controlled laboratory conditions at the Institute of Nuclear Sciences "Vinča", Belgrade, Serbia. EPAD was irradiated at six different dose rates with the same absorbed dose (Fig. 6), and after each irradiation step, there was a reprogramming step. After that phase the same EPAD was irradiated with nine more cycles of the highest dose rate (Fig. 7).

During each cycle, the component received the same absorbed dose of 470 mGy. The sensitivity of floating gate dosimeters decreases with

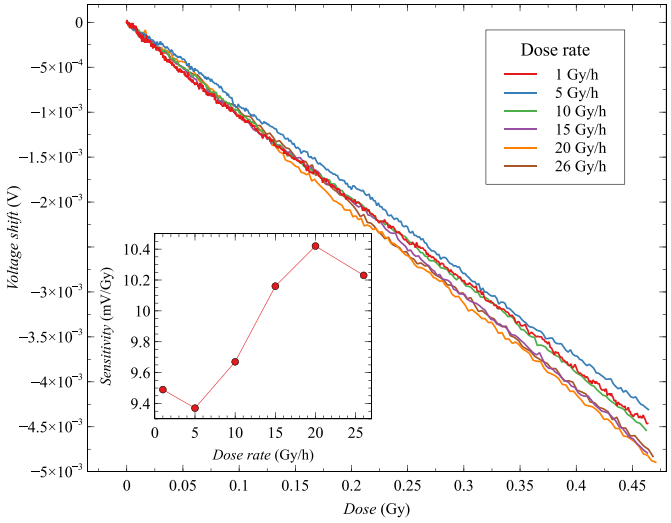

Fig. 6. Dependence of Δ*Vth* on absorbed dose at six different dose rates.

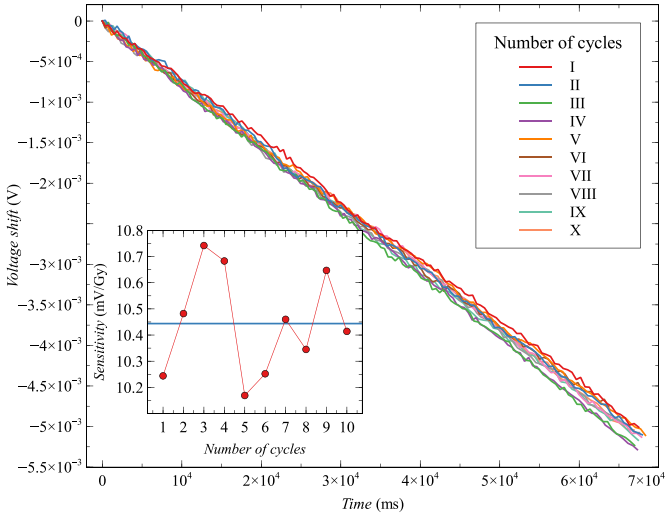

Fig. 7. Ten cycles of irradiation at 26 Gy/h dose rate.

discharging of the floating gate during irradiation [20]. Reprogramming has the role of returning the transistor to the initial value of the threshold voltage so that in each cycle the transistor has the same starting point.

In Fig. 6 a change in slope for different dose rates can be observed. From 5 to 20 Gy/h an approximately linear increase of EPAD sensitivity is noticed. On the other hand, in Fig. 7 where is a constant dose rate of 26 Gy/h for ten cycles, the sensitivity value of EPAD oscillates around a mean value of 10.44 mV/Gy with a standard deviation of 0.19 mV/Gy. If we now analyze in more detail the dependence of EPAD sensitivity on the dose rate from Fig. 6 with the added error from the calculated standard deviation (presented in Fig. 8), it can be concluded that the sensitivity of EPAD has a tendency to increase with the dose rate. In the absence of results, the standard deviation value for the highest dose rate was taken for other values to give an impression of the magnitude of errors that may occur and determine whether there is a tendency of increasing the sensitivity of the component with the dose rate.

Threshold voltage shift (drift) before and after the irradiation step at 26 Gy/h dose rate is shown in Fig. 9.

It clearly can be distinguished when the radiation source is turned on and when it is off. The threshold voltage shift during irradiation is linear because of the low absorbed dose. Analysing the threshold voltage shift

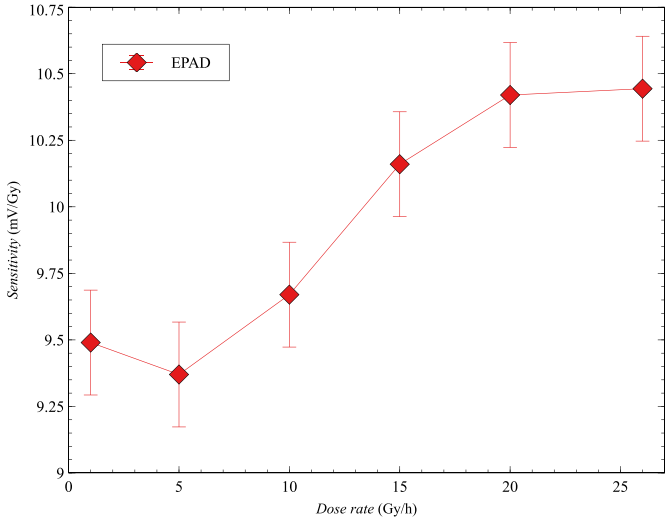

Fig. 8. Dependence of EPAD sensitivity on the dose rate.

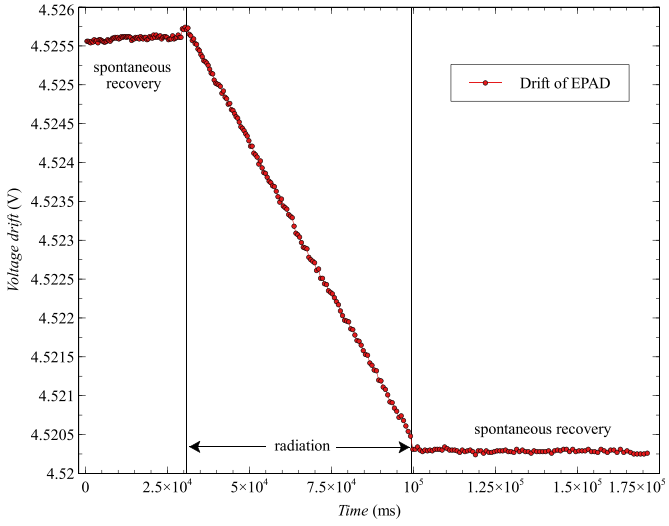

Fig. 9. Drift before and after the irradiation step at 26 Gy/h dose rate.

(drift) after the absorbed doses of 0.46 Gy, 2.78 Gy and 7.64 Gy in the Fig. 10 no difference can be observed. However, compared with the threshold voltage shift immediately after a non-irradiated device's programming process, a more considerable drift can be observed. It can also be noticed that the threshold voltage shift value after absorbed doses saturates to an average value of 0.06 mV for the first 80 s.

One of the most important characteristics of dosimeters is the minimum dose that can be detected. We have calculated the minimum detectable dose to be 52 mGy at a signal to noise ratio of 5. The noise was estimated from the maximum residual error of the linear fit to the sensitivity data. Fig. 11 shows the measured data for a dose rate of 1 Gy/h and linear fitting function for the absorbed dose of 52 mGy.

This noise comprises the voltage resolution of the measurement instrument. How all measurements of the transistor were performed at its zero temperature coefficient point of 64 *A* the temperature drift can be neglected. The component sensitivity for this dose rate was calculated as 9.49 mV/Gy, considering the saturated drift value of 0.06 mV, the minimum value of the absorbed dose uncertainty was obtained to be 6.32 mGy which is 12.15% of the minimum detectable dose.

Irradiation and recharging steps for ten cycles with the constant dose rate are shown in Fig. 12. The reprogramming characteristic is not degrading with the absorbed dose because the programming time is within an acceptable range determined on pristine devices. Reprogramming characteristic can be defined as the time required to reach the set value from the initial value of the threshold voltage by charging the floating gate with electrons by programming electronics system.

Non-ideality in the reprogramming characteristic, which can be seen in Fig. 12, such as overshoots or undershoots of the programmed threshold voltage values, are a consequence of bad value readings, which were later solved by software. The problem lies in reading threshold voltage value several times in a row, and bad values such as overshoots or undershoots are not taken as the real threshold voltage value. Unfortunately, this problem was later noticed, so in these results, a higher or lower threshold voltage value at the beginning of the new cycle can be seen.

5. Discussion

Comparing the drift values after programming the non-irradiated component with the drift values after irradiation, it can be observed that the drift value is greater after programming than after irradiation, which means that structural defects during irradiation are significantly smaller than the residual charge that occurs after programming, which shows that this component due to its special floating gate design is well

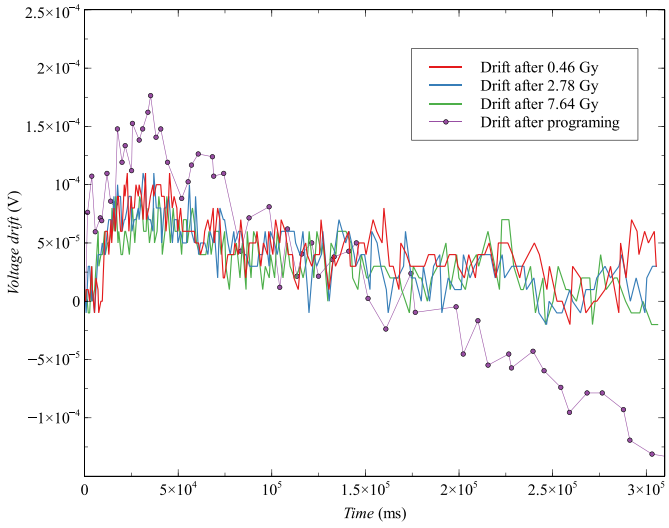

Fig. 10. Threshold voltage drift after different absorbed doses.

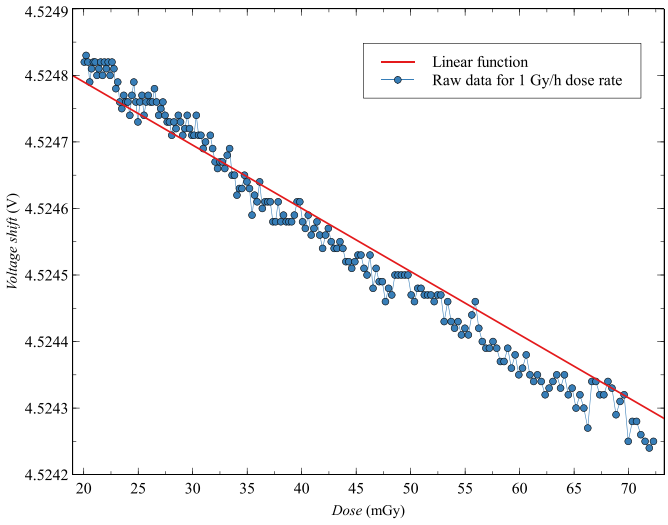

Fig. 11. Threshold voltage shift for minimum detectable dose.

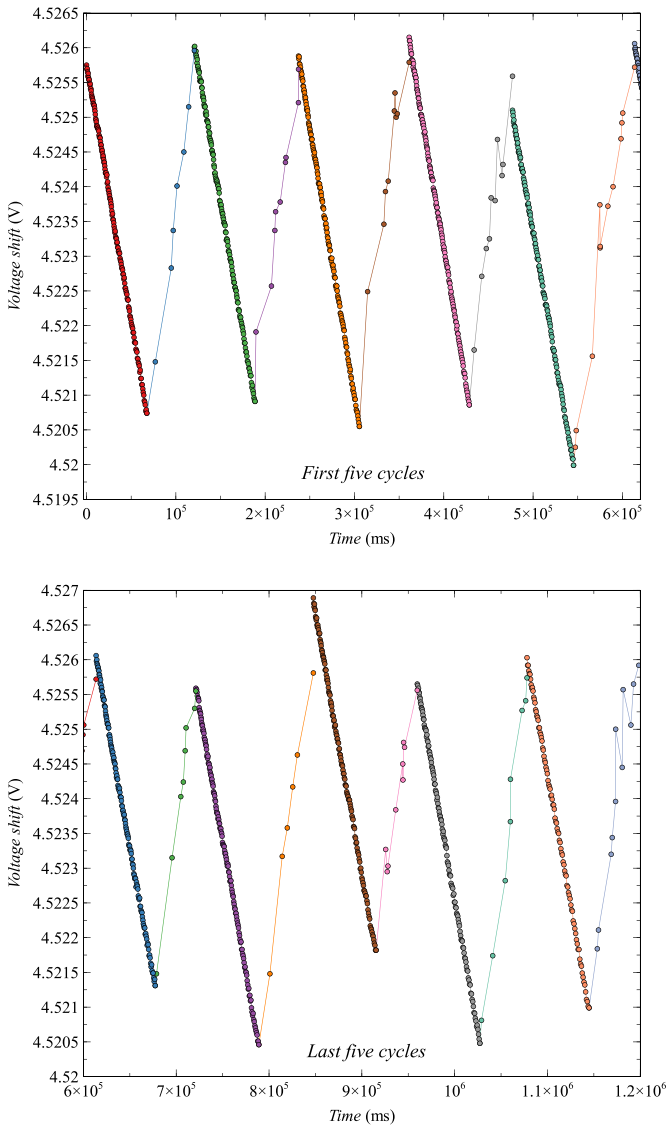

Fig. 12. Ten cycles of irradiation and recharging with the 26 Gy/h dose rate.

resistant to defects caused by gamma radiation.

In this paper, it was found that the reprogramming characteristic does not change during the reprogramming cycles, which indicates that are no defects created in the tunnel oxide of the charging transistor that can create electron scattering and increase programming time, which was observed for higher absorbed doses in the earlier publication [19].

One of the most exciting results is the dependence of EPAD sensitivity on the dose rate. The group at CERN also measured an increase in the sensitivity of the floating gate dosimeter for a higher dose rate, which can be seen in the paper [14] (Fig. 2). To the best of our knowledge, we did not find an explanation for this phenomenon in the literature. Based on the results, we can conclude that a larger amount of photons per unit of time (high dose rate) excites a larger amount of electrons than the same amount of photons would do in a longer period (low dose rate). For a higher dose rate more energy is deposited in the material per unit time than for a lower dose rate, and therefore it can be concluded that at higher deposited energy per unit time more electrons get enough energy to overcome the energy barrier of the floating gate than at lower deposited energy for the same total deposited energy (absorbed dose).

However, the sensitivity value of EPAD during ten cycles with the same dose rate shows no tendency to increase or decrease. Value oscillations during repetition indicate the sensitivity error needs to be calculated in the final absorbed dose reading of this dosimeter. On the other hand, this result shows what the group at CERN with its custom floating gate sensor also showed [14], that semiconductor sensors with a floating gate structure can be used multiple times with the same dosimetric characteristic, which is very important for the application of these dosimeters.

EPAD has very promising features compared to other commercial floating gate-based components such as Flash Memories. It has been shown that a Flash memory chip in 20 nm technology can detect an absorbed dose of 1*Gy* [27]. Further tests of the reliability of the EPAD, the maximum number of cycles, the influence of the dose rate on the sensitivity at a larger dose rate range and the degradation of the reprogramming characteristic at higher absorbed doses need to be done.

The requirements of a professional dosimeter are detection as low as possible minimum detectable dose, very accurate dose readings at the position where it is worn or placed, reading in the field in real-time so user can avoid the dose of concern, miniature dimensions, minimal maintenance, reproducibility, operating in a low power mode and independent of the harsh environmental conditions such as temperature, humidity and pressure [28].

Semiconductor dosimeters have miniature dimensions and therefore can have accurate dose readings at the position they are worn or placed if they are monolithically integrated with a reading circuit [15] or work in a passive regime measurement. They are also maintenance-free, tends to be low-power, and with military-grade quality packaging can be protected from certain environmental conditions, such as humidity and pressure. The dose value reading can be temperature independent if certain properties of the semiconductor component are used, such as the zero temperature coefficient point (ZTC) for MOSFET based dosimeters [29]. Comparison of four most common semiconductor dosimeters is given in Table 1.

The PIN diode cannot be used as a passive dosimeter because it is used in current mode, so its output current depends on the dose rate [32]. The highest sensitivity of the PIN diode is with the reverse bias when there is a complete depletion of the intrinsic region. Temperature independent of the device is long as the reverse bias voltage exceeds the saturation voltage [33]. pMOS dosimeter (RADFET) is a transistor with thick oxide, which is sensitive to radiation due to the generation of electron-hole pairs in the thick oxide. The holes remain trapped in the oxide, and their electric field causes the threshold voltage to shift. It is most sensitive to positive bias at the gate, and it can work at zero temperature coefficient point (ZTC) and thus be independent of the temperature influence; due to the very thick oxide (1 μm), it cannot be monolithically integrated with other circuits. Also, RADFETs cannot be reused [31,34,35]. Direct Ion Storage (DIS) is a hybrid of ion chamber and floating gate MOSFET. The operating voltage of the ionizing chamber is 25 to 30 V. Due to the complex design it is not CMOS compatible. Its advantages are very high sensitivity and reusability [5,30].

Floating gate (FG) dosimeters have the highest sensitivity at zero gate bias; the influence of ambient temperature can be eliminated by operating at its zero temperature coefficient (ZTC) point [20]. They can be incorporated into standard CMOS processes due to the thin oxides in

Table 1
Formal comparison table for semiconductor dosimeters.

	PIN	pMOS	DIS	FG
Minimum Detectable Dose	–	2 rad (SiO_2) [31]	10 μSv [30]	5.2 rad (H_2O)
Temp. independent real-time reading	Yes	Yes	–	Yes
Passive measurement	No	Yes	Yes	Yes
Highest sensitivity with zero bias	No	No	No	Yes
Reproducibility	Yes	No	Yes	Yes
Monolithic integration (CMOS compatibility)	No	No	No	Yes

their structure [12]. FG have reproducibility because it can be used multiple times with the same dosimetric characteristic. The minimum detectable dose of commercial floating gate structure (EPAD) that can be measured in real-time is about 50 mGy. However, this parameter can be improved by the special design of this component with a larger active area of the floating gate.

6. Conclusion

EPAD shows the same dosimetric characteristics during ten irradiation cycles. An increase of EPAD sensitivity with the dose rate was observed. There is no change in the drift of the EPAD after the irradiation cycles, which indicates a negligible amount of electron-hole pairs that remain trapped in the oxide or at the interface between oxide and channel of the main transistor. The minimal detectable dose has calculated to be the 52 mGy at a signal to noise ratio of 5. Based on the results, it can be concluded that this floating gate device's characteristics have great potential for dosimetry applications and may tend to professional level's requirements in the future.

CRediT authorship contribution statement

Conception and design of study: S.D. Ilic, G.S. Ristic, M.S. Andjelkovic, R. Duane;

Acquisition of data: S.D. Ilic, S. Stankovic;

Analysis and/or interpretation of data: S.D. Ilic, M. Sarajlic, A.J. Palma.

Drafting the manuscript: S.D. Ilic, M. Sarajlic, G.S. Ristic;

Revising the manuscript critically for important intellectual content: M.S. Andjelkovic, R. Duane,

S. Stankovic, A.J. Palma.

Approval of the version of the manuscript to be published (the names of all authors must be listed):

S.D. Ilic, M.S. Andjelkovic, R. Duane, A.J. Palma, M. Sarajlic, S. Stankovic, G.S. Ristic.

Declaration of competing interest

The authors have no affiliation with any organization with a direct or indirect financial interest in the subject matter discussed in the manuscript.

Acknowledgment

This research was funded by Ministry of Education, Science and Technological Development of the Republic of Serbia, under the project No.43011, grant No.451-03-9/2021-14/200026 and European Commission, WIDESPREAD-2018-3-TWINNING, grant No.857558 - ELICSIR.

References

[1] M. Prokic, Thermoluminescent characteristics of calcium sulphate solid detectors, Radiat. Prot. Dosim. 37 (4) (1991) 271–274, https://doi.org/10.1093/oxfordjournals.rpd.a081062.

[2] A. Holmes-Siedle, The space-charge dosimeter: general principles of a new method of radiation detection, Nucl. Inst. Methods 121 (1) (1974) 169–179, https://doi.org/10.1016/0029-554X(74)90153-0.

[3] G.S. Ristic, Influence of ionizing radiation and hot carrier injection on metal-oxide-semiconductor transistors, J. Phys. D. Appl. Phys. 41 (2) (2008), 023001, https://doi.org/10.1088/0022-3727/41/2/023001.

[4] G.S. Ristic, M. Andjelkovic, A.B. Jaksic, The behavior of fixed and switching oxide traps of RADFETs during irradiation up to high absorbed doses, Appl. Radiat. Isot. 102 (2015) 29–34, https://doi.org/10.1016/j.apradiso.2015.04.009.

[5] J. Kahilainen, The direct ion storage dosemeter, Radiat. Prot. Dosim. 66 (1–4) (1996) 459–462, https://doi.org/10.1093/oxfordjournals.rpd.a031778.

[6] V. Mathur, Ion storage dosimetry, Nucl. Inst. Methods Phys. Res. B 184 (1) (2001) 190–206, https://doi.org/10.1016/S0168-583X(01)00714-5. Advanced Topics in Solid State Dosimetry.

[7] Y. Xuan, C. Mousoulis, A. Kumar, C.I. Elmiger, S. Scott, D.J. Valentino, D. Peroulis, 3D MOS-capacitor-based ionizing radiation sensors, in: 2017 IEEE Sensors, 2017, pp. 1–3, https://doi.org/10.1109/ICSENS.2017.8234043.

[8] N.G. Tarr, G.F. Mackay, K. Shortt, I. Thomson, A floating gate MOSFET dosimeter requiring no external bias supply, in: RADECS 97. Fourth European Conference on Radiation and its Effects on Components and Systems (Cat. No.97TH8294), 1997, pp. 277–281, https://doi.org/10.1109/RADECS.1997.698909.

[9] E. Pikhay, Y. Roizin, Y. Nemirovsky, Ultra-low power consuming direct radiation sensors based on floating gate structures, J. Low Power Electron. Appl. 7 (3) (2017) 20, https://doi.org/10.3390/jlpea7030020.

[10] J. Bi, Radiation effects of floating-gate (FG) and charge-trapping (CT) Flash memory technologies, in: 2019 International Conference on IC Design and Technology (ICICDT), 2019, pp. 1–3, https://doi.org/10.1109/ICICDT.2019.8790893.

[11] B. Chatterjee, C. Mousoulis, D. Seo, A. Kumar, S. Maity, S.M. Scott, D.J. Valentino, D.T. Morisette, D. Peroulis, S. Sen, A wearable real-time cmos dosimeter with integrated zero-bias floating gate sensor and an 861-nw 18-bit energy-resolution scalable time-based radiation to digital converter, IEEE J. Solid State Circuits 55 (3) (2020) 650–665, https://doi.org/10.1109/JSSC.2019.2953833.

[12] E. Garcia-Moreno, E. Isern, M. Roca, R. Picos, J. Font, J. Cesari, A. Pineda, Floating gate CMOS dosimeter with frequency output, IEEE Trans. Nucl. Sci. 59 (2) (2012) 373–378, https://doi.org/10.1109/TNS.2012.2184301.

[13] S. Danzeca, J. Cesari, M. Brugger, L. Dusseau, A. Masi, A. Pineda, G. Spiezia, Characterization and modeling of a floating gate dosimeter with gamma and protons at various energies, IEEE Trans. Nucl. Sci. 61 (6) (2014) 3451–3457, https://doi.org/10.1109/TNS.2014.2364274.

[14] M. Brucoli, S. Danzeca, M. Brugger, A. Masi, A. Pineda, J. Cesari, L. Dusseau, F. Wrobel, Floating gate dosimeter suitability for accelerator-like environments, IEEE Trans. Nucl. Sci. 64 (8) (2017) 2054–2060, https://doi.org/10.1109/TNS.2017.2681651.

[15] M. Brucoli, J. Cesari, S. Danzeca, M. Brugger, A. Masi, A. Pineda, L. Dusseau, F. Wrobel, Investigation on passive and autonomous mode operation of floating gate dosimeters, IEEE Trans. Nucl. Sci. 66 (7) (2019) 1620–1627, https://doi.org/10.1109/TNS.2019.2895366.

[16] R. Edgecock, J. Matheson, M. Weber, E.G. Villani, R. Bose, A. Khan, D. Smith, I. Adil-Smith, A. Gabrielli, Evaluation of commercial programmable floating gate devices as radiation dosimeters, J. Instrum. 4 (02) (2009) P02002, https://doi.org/10.1088/1748-0221/4/02/P02002.

[17] R. Bose, The Development of an In-vivo Dosimeter for the Application in Radiotherapy, Citeseer, 2012. Ph.D. thesis.

[18] ALD, QUAD/DUAL electrically programmable analog device, URL, http://www.aldinc.com/pdf/ALD1110E.pdf, 2012.

[19] S. Ilic, A. Jevtic, S. Stankovic, V. Davidovic, Feasibility of applying an electrically programmable floating-gate MOS transistor in radiation dosimetry, in: Proceedings IEEE 31st International Conference On Microelectronics, IEEE Serbia and Montenegro Section - ED/SSC Chapter, 2019, pp. 67–70, https://doi.org/10.1109/MIEL.2019.8889570.

[20] S. Ilic, A. Jevtic, S. Stankovic, G. Ristic, Floating-gate MOS transistor with dynamic biasing as a radiation sensor, Sensors 20 (11) (2020) 3329, https://doi.org/10.3390/s20113329.

[21] G. Ristic, S. Golubovic, M. Pejovic, Sensitivity and fading of pMOS dosimeters with thick gate oxide, Sensors Actuators A Phys. 51 (2) (1996) 153–158, https://doi.org/10.1016/0924-4247(95)01211-7.

[22] E.S. Snyder, P.J. McWhorter, T.A. Dellin, J.D. Sweetman, Radiation response of floating gate EEPROM memory cells, IEEE Trans. Nucl. Sci. 36 (6) (1989) 2131–2139, https://doi.org/10.1109/23.45415.

[23] S. Gerardin, A. Paccagnella, Present and future non-volatile memories for space, IEEE Trans. Nucl. Sci. 57 (6) (2010) 3016–3039, https://doi.org/10.1109/TNS.2010.2084101.

[24] J.W. Eaton, D. Bateman, S. Hauberg, R. Wehbring, GNU Octave Version 4.4.0 Manual: A High-level Interactive Language for Numerical Computations, 2018.

[25] P.J. McWhorter, P.S. Winokur, Simple technique for separating the effects of interface traps and trapped-oxide charge in metal-oxide-semiconductor transistors, Appl. Phys. Lett. 48 (2) (1986) 133–135, https://doi.org/10.1063/1.96974.

[26] ALD, Application note ALD1108, 1998.

[27] P. Kumari, L. Davies, N.P. Bhat, E.X. Zhang, M.W. McCurdy, D.M. Fleetwood, B. Ray, State-of-the-art flash chips for dosimetry applications, in: 2018 IEEE Radiation Effects Data Workshop (REDW), IEEE, 2018, pp. 1–4.

[28] Radiation Emergency Medical Management, Eight categories of radiation dosimeters for dose and exposure monitoring and worker safety, URL, https://www.remm.nlm.gov/radiation-dosimeters-dose-monitoring-worker-safety.htm, May 2021.

[29] Z. Prijic, S. Dimitrijev, N. Stojadinovic, The determination of zero temperature coefficient point in CMOS transistors, Microelectron. Reliab. 32 (6) (1992) 769–773, https://doi.org/10.1016/0026-2714(92)90041-I.

[30] C. Wernli, Dosimetric characteristics of a novel personal dosemeter based on direct ion storage (DIS), Radiat. Prot. Dosim. 66 (1–4) (1996) 23–28, https://doi.org/10.1093/oxfordjournals.rpd.a031724.

[31] A. Holmes-Siedle, L. Adams, Radfet: a review of the metal-oxide-silicon devices as dosimeters use of integrating, Radiat. Phys. Chem. 28 (2) (1986) 235–244, https://doi.org/10.1016/1359-0197(86)90134-7.

[32] R. Kumar, S. Sharma, A. Philomina, A. Topkar, Dosimetric characteristics of a pin diode for radiotherapy application, Technol. Cancer Res. Treat. 13 (4) (2014) 361–367, https://doi.org/10.7785/tcrt.2012.500388.

[33] Microsemi Corporation,.URL https://www.microsemi.com/sites/default/files/datasheets/Products/rf/APPENDIX.
[34] A. Jaksic, Y. Kimoto, A. Mohammadzadeh, A. Mathewson, Dose rate dependence of RADFET irradiation and post-irradiation responses, in: 2004 24th International Conference on Microelectronics (IEEE Cat. No.04TH8716) Vol. 2, 2004, pp. 661–664, https://doi.org/10.1109/ICMEL.2004.1314915.
[35] J. Mekki, M. Brugger, S. Danzeca, L. Dusseau, K. Røed, G. Spiezia, Mixed particle field influence on RadFET responses using co-60 calibration, IEEE Trans. Nucl. Sci. 60 (4) (2013) 2435–2443, https://doi.org/10.1109/TNS.2013.2253800.